Solvent Codeposition and Cis−Trans Isomerization of Isophthalic Acid Derivatives Studied by STM

P. Vanoppen, P. C. M. Grim, M. Rücker, S. De Feyter, G. Moessner,† S. Valiyaveettil,† K. Müllen,† and F. C. De Schryver*

University of Leuven (KUL), Department of Chemistry, Laboratory of Molecular Dynamics and Spectroscopy, Celestijnenlaan 200-F, 3001 Heverlee, Belgium

Received: September 9, 1996[⊗]

Scanning tunneling microscopy (STM) was used to study physisorbed monolayers of 5-octadecyloxyisophthalic acid (C_{18}ISA) and 5-[ω-(4′-dodecyloxy-4-azobenzeneoxy)dodecyloxy]isophthalic acid (C_{12}(AZO)C_{12}ISA) at a liquid/graphite interface. The acquired STM images exhibit the molecular packing of the monolayers with submolecular resolution. Monolayers formed by codeposition of solvent molecules and C_{18}ISA or C_{12}(AZO)C_{12}-ISA molecules are found when 1-octanol and 1-undecanol are used as a solvent. The cis and trans isomers of C_{12}(AZO)C_{12}ISA, the reagent and reaction product of a reversible photoinduced reaction, are simultaneously present and are both structurally identified at the liquid/graphite interface.

Introduction

Scanning tunneling microscopy (STM) was already successfully applied for imaging a wide range of physisorbed two-dimensional organic films on a graphite surface.[1−4] Various aspects of physisorbed organic monolayers at the liquid/solid interface have been investigated including domain dynamics,[5−10] codeposition of two-component alcohol mixtures,[11,12] and a chemical reaction.[13]

Recently, certain properties of the class of isophthalic acid derivatives were investigated such as their liquid crystalline behavior[14] and self-assembly in the solid state.[15−17] Moreover, STM was employed to investigate monolayers of 5-hexadecyloxyisophthalic acid (C_{16}ISA) molecules at the liquid/graphite interface. The obtained 2D structure of their packing was compared with the 3D crystal structure determined by X-ray analysis.[19]

In this paper we present a STM study of 5-octadecyloxyisophthalic acid (C_{18}ISA) and 5-[ω-(4′-dodecyloxy-4-azobenzenexy)dodecyloxy]isophthalic acid (C_{12}(AZO)C_{12}ISA), which self-assemble at a liquid/graphite interface in a reproducible fashion. The chemical structure of the compounds is depicted in Figure 1.

We focused on the structural investigation of physisorbed monolayers using solvents capable of hydrogen bond formation with the isophthalic acid groups. We report for the first time codeposition of solvent molecules with isophthalic acid derivatives and cis−trans isomerization of the azobenzene-containing C_{12}(AZO)C_{12}ISA. The cis and trans isomers, respectively reagent and product of a photoinduced reversible reaction, are structurally identified at the liquid/graphite interface.

Experimental Section

The synthesis of C_{18}ISA was reported previously.[20] C_{12}-(AZO)C_{12}ISA was synthesized following in sequence the steps a−e described below.

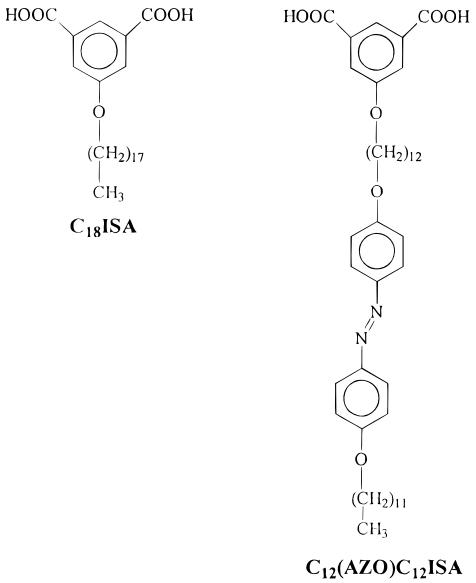

Figure 1. Chemical structure of C_{18}ISA and C_{12}(AZO)C_{12}ISA.

(a) Dimethyl 5-(ω-bromododecyloxy)isophthalate (1). 1,-12-dibromododecane (8.0 g, 0.024 mol), powdered K_2CO_3 (3.31 g, 0.024 mol), a catalytic amount of KI, and 80 mL of dry *N*,*N*-dimethylformamide were placed in a two-necked round-bottom flask equipped with a reflux condensor, a pressure-equalizing funnel, and a magnetic stirrer. The mixture was stirred and heated to 80 °C. Dimethyl 5-hydroxyisophthalate (2.56 g, 0.012 mol) in 30 mL of dry *N*,*N*-dimethylformamide was added dropwise over a period of 6 h. After the mixture was stirred for another 10 h at 80 °C, the solvent was removed. The crude product was taken up in dichloromethane and twice washed with water. After the organic fraction was dried over magnesium sulfate and dichloromethane removed, the obtained product was purified by column chromatography on silica gel (eluent: ethyl acetate/*n*-heptane (1:5)). The pure product is white and crystalline. Yield: 3.1 g (56%). ^{1}H NMR ($CDCl_3$): δ 8.26 (s, 1 H), 7.73 (s, 2 H), 4.05 (t, 2 H, J = 3 Hz), 3.95 (s, 6 H), 3.41 (t 2 H, J = 4 Hz), 1.94−1.72 (m, 4 H), 1.62−1.23 (m, 16 H). ^{13}C NMR ($CDCl_3$): δ 166.6, 159.7, 132.2 (2), 123.2 (2), 120.3 (2),

† Max-Planck Institute for Polymer Research, P.O. Box 3148, D-55021 Mainz, Germany.

* To whom correspondence should be addressed.

[⊗] Abstract published in *Advance ACS Abstracts,* November 1, 1996.

S0022-3654(96)02737-2 CCC: $12.00

76.9, 69.1, 52.8, 34.4, 33.3, 30.0, 29.9, 29.8, 29.6, 29.2, 28.6, 26.4. EI-MS: *m*/*z* 458.1 [(M + 1)$^+$].

(b) 4,4′-Dihydroxyazobenzene (2). 4-Hydroxyanilin (6.4 g, 0.058 mol) was dissolved in 100 mL of dilute hydrochloric acid (1 M) and cooled to 0 °C. An aqueous solution of sodium nitrite (4.03 g, 0.058 mol in 20 mL of water) was added dropwise under constant stirring. The mixture is diluted by adding 200 mL of precooled methanol. In a separate batch, phenol (5.46 g, 0.058 mol) and potassium hydroxide (6.2 g, 0.11 mol) are dissolved in 40 mL of methanol and also cooled to 0 °C. This phenolate solution is added dropwise under constant stirring to the first mixture. The red solution is stirred for another 2 h at 0 °C before the reaction is quenched with dilute hydrochloric acid. The red solid was filtered, washed thoroughly with water, and dried. The crude material was purified by recrystallization from concentrated acetic acid. Yield: 4.48 g, 0.021 mol, 36%. ^{1}H NMR: (DMSO-d_6) δ 10.05 (br, 2 H), 7.74 (d, 4 H, J = 4 Hz), 6.93 (d, 4 H, J = 4 Hz); ($CDCl_3$) δ 7.84 (d, 4 H, J = 4 Hz), 6.95 (d, 4 H, J = 4 Hz), 5.05 (br, 2 H). ^{13}C NMR (DMSO-d_6): δ 160.3 (2), 145.6 (2), 124.4 (4), 116.1 (4). EI-MS: *m*/*z* 214.0 (M$^+$).

(c) 4-Hydroxy-4′-dodecyloxyazobenzene (3). 4,4′-Dihydroxyazobenzene (4.3 g, 0.02 mol) was mixed with powdered K_2CO_3 and a catalytic amount of KI, and the mixture was suspended in 80 mL of dry *N*,*N*-dimethylformamide as described in procedure a. A solution of 1-bromododecane (2.72 g, 0.011 mol) in 30 mL of dry *N*,*N*-dimethylformamide was added dropwise to the mixture and stirred for 10 h at 80 °C. The workup was done as described above. The yellow product was purified by column chromatography on silica gel (eluent: ethyl acetate/*n*-heptane (1:1)) to obtain the pure monoalkylated product (**3**). Yield: 2.9 g (0.0076 mol, 69.5%) (**3**). ^{1}H NMR ($CDCl_3$): δ 7.86 (dd, 4 H, J = 5 Hz, 4 Hz), 6.99 (dd, 4 H, J = 7 Hz, 5 Hz), 5.62 (br, 1 H), 4.05 (t, 2 H, J = 3 Hz), 1.94−1.75 (m, 2 H), 1.57−1.12 (m, 18 H), 0.90 (t, 3 H, J = 2.5 Hz). ^{13}C NMR ($CDCl_3$): δ 161.8, 158.1, 147.7, 147.4, 125.0 (2), 124.8 (2), 116.2 (2), 115.2 (2), 66.9, 32.4, 30.0 (3), 29.8 (3), 29.7, 26.5, 23.1, 14.6. FD-MS: *m*/*z* 383.4 [(M+1)$^+$].

(d) Dimethyl 5-[(ω-4′-dodecyloxy-4-azobenzeneoxy)dodecyloxy]isophthalate (4). The ω-bromodiester (**1**, 1.4 g, 0.0031 mol) and the phenol (**3**, 1.17 g, 0.0031 mol) were mixed with 2.5 equivalents of powdered K_2CO_3 and suspended in dry *N*,*N*-dimethylformamide. The mixture is stirred at 80 °C for 12 h. After most of the solvent was removed, the residue was taken in dichloromethane and purified as described in step a. Purification of the crude material was achieved by repeated recrystallization from methanol. Yield: 1.6 g (0.021 mol, 68%). ^{1}H NMR ($CDCl_3$): δ 8.28 (s, 1 H), 7.88 (d, 4 H, J = 4 Hz), 7.72 (s, 2 H), 6.99 (d, 4 H, J = 4 Hz), 4.04 (t, 6 H, J = 3 Hz), 3.94 (s, 6 H), 1.90−1.68 (m, 6 H), 1.62−1.16 (m, 34 H), 0.88 (t, 3 H, J = 2.5 Hz). ^{13}C NMR ($CDCl_3$): δ 166.6, 161.7, 159.7, 147.5, 132.2, 124.8, 123.2, 120.2, 115.2, 76.9, 69.1, 52.8, 32.4, 30.0, 29.9, 29.7, 29.6, 29.2, 28.6, 26.5, 23.1, 14.6. FD-MS: *m*/*z* 759.2 [(M+1)$^+$].

(e) C_{12}(AZO)C_{12}ISA (5). The methyl ester (**4**) (1.3 g, 0.0017 mol) was hydrolyzed by refluxing it with 3.5 equivalents of potassium hydroxide in a mixture of ethanol and water (2:1) for 8 h. After evaporation of the alcohol, the alkaline aqueous solution was rendered neutral using dilute hydrochloric acid (10 M) up to a pH of 4−5. The product precipitated as a yellow solid, which was extracted from the aqueous phase with diethyl ether. The organic phase was washed twice with water and dried over magnesium sulfate. The obtained crude acid after evaporation of diethyl ether was purified by double recrystallization from methanol. Yield: 0.88 g (0.0012 mol, 70.6%). ^{1}H NMR (DMSO-d_6): δ 8.09 (s, 1 H), 7.85 (d, 4 H, J = 4 Hz), 7.66 (s, 2 H), 7.09 (d, 4 H, J = 4 Hz), 4.08 (t, 6 H, J = 3 Hz), 1.85−1.62 (m, 6 H), 1.51−1.15 (m, 34 H), 0.89 (t, 3 H, J = 2.5 Hz). ^{13}C NMR (DMSO-d_6): δ 166.7, 161.2, 159.1, 156.3, 132.9, 124.8, 123.7, 119.3, 115.2, 77.2, 68.4, 55.6, 32.4, 30.7, 30.0, 29.8, 29.6, 29.2, 28.8, 26.5, 25.6, 23.2, 14.6. FD-MS: *m*/*z* 731.9 [(M+1)$^+$]

The steps a, b, and d were conducted under a dry argon atmosphere. ^{1}H and ^{13}C NMR spectra were recorded on a Varian Gemini 200 spectrometer. Chemical shifts are reported in parts per million (ppm) and are referenced to residual proton-containing solvent (δ($CDCl_3$) = 7.26; δ(DMSO-d_6) = 2.49). Mass spectra were determined on a ZAB2-SE-FPD instrument. All commercially available reagents were used without further purification.

STM experiments were performed using a Discoverer scanning tunneling microscope (TopoMetrix Inc., Santa Barbara, CA) along with an external pulse/function generator (Model HP 8111 A). Tips are electrochemically etched from Pt/Ir wire (80%/20%, diameter 0.2 mm) in 2 N KOH/6 N NaCN solution in water.

Prior to STM experiments, the compound under investigation was dissolved in a solvent with a high boiling point. The solvents employed were 1-phenyloctane (Aldrich, 99%), 1-octanol (Sigma, 99.6%), and 1-undecanol (Aldrich, 99%). Concentrations used were typically about 1 mg/mL. Samples were prepared by spreading a drop of this solution on the basal plane of highly ordered pyrolytic graphite (HOPG) (grade ZYB, Advanced Ceramics Inc., Cleveland, OH).

All the presented STM images were acquired in the variable current mode (constant height) under ambient conditions. The speed of image acquisition was relatively slow. For example, for an image consisting of 200 lines and 200 pixels per line, approximately 7 s was the minimum acquisition time for one image frame, which is limited by the Discoverer instrument. Typically, a tunneling current of 1 nA and a bias voltage of 0.5−1.5 V referenced to the graphite surface were employed. STM images obtained at low bias voltages reliably revealed the atomic structure of HOPG, providing an internal calibration standard for the monolayer studies. The presented STM data were not subjected to image processing.

Irradiation of the solution in a cuvette as well as on the graphite surface was performed using a CAMAG universal lamp with a wavelength of 366 nm.

Results and Discussion

Solvent Codeposition. Figure 2a shows a STM image of a monomolecular layer of C_{18}ISA adsorbed from a C_{18}ISA solution in 1-phenyloctane applied to the basal plane of HOPG. The image reveals a closely packed arrangement of C_{18}ISA molecules on the graphite surface with submolecular resolution. The functional groups of C_{18}ISA molecules can clearly be recognized. The bright spots appearing in the image can be correlated with the isophthalic acid groups of the molecule. Bright and dark refers to the black/white contrast in the images. White corresponds to the highest and black to the lowest measured tunneling current in the image. The occurrence of a higher tunneling current above an aromatic moiety, as predicted by theoretical calculations,[21] is a general finding, which has been observed for a large variety of organic adsorbates on graphite. The darker regions in the image correspond to the alkyl groups of the molecules.

On the basis of the found monolayer structure, a 2D unit cell and an illustrative molecular model (Figure 2b) for the molecular arrangement could be proposed. The unit cell as marked in

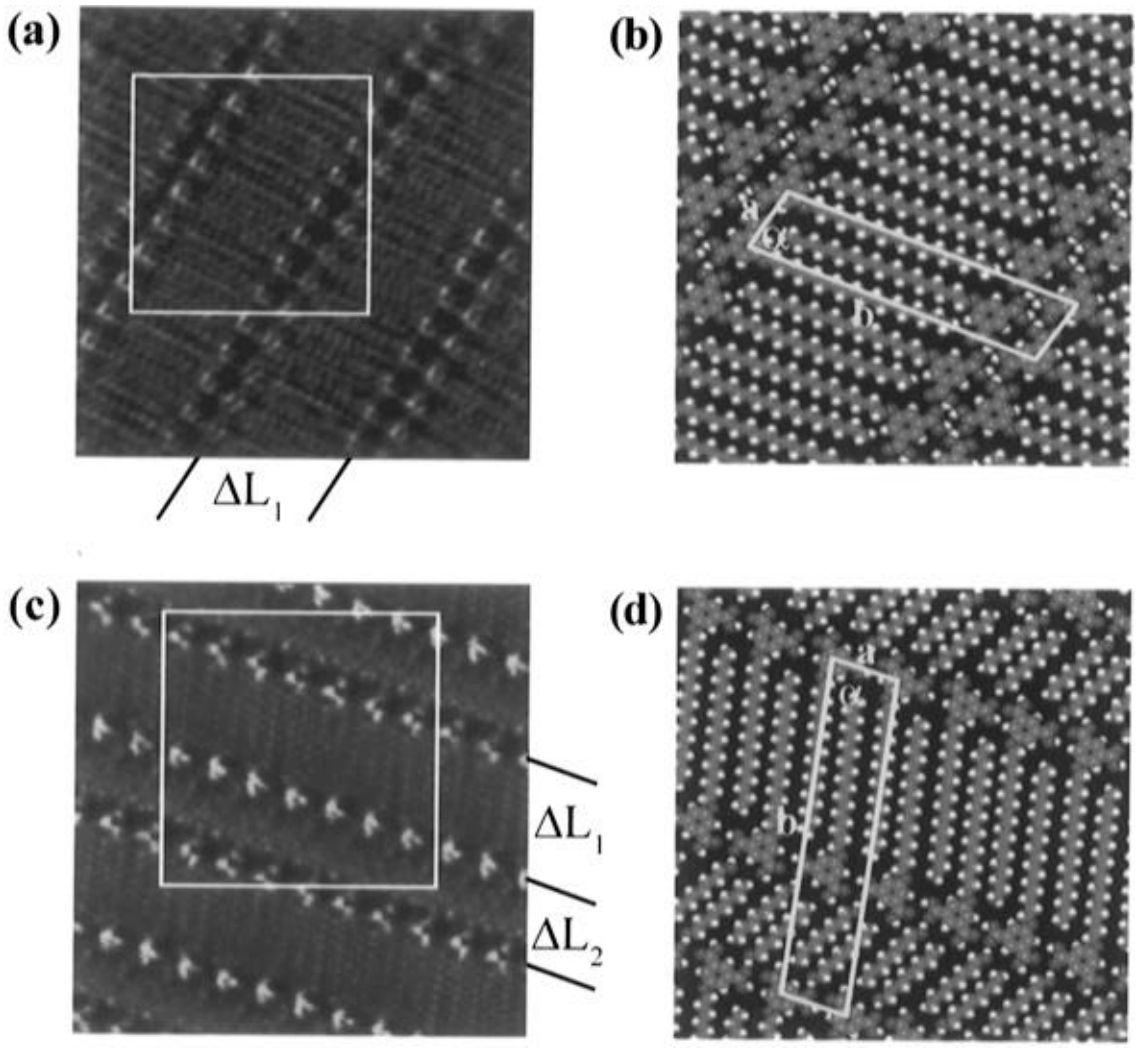

Figure 2. (a) STM image of an ordered monolayer of C_{18}ISA molecules formed by physisorption from 1-phenyloctane at a liquid/graphite interface. Image size is 10.7 × 10.7 nm^2. ΔL_1 is the width of one lamella of interdigitated C_{18}ISA molecules. (b) Molecular model for the two-dimensional packing of C_{18}ISA molecules and proposed unit cell. The unit cell contains two C_{18}ISA molecules. The molecular model represents the area indicated in the STM image. (c) STM image of an ordered monolayer of C_{18}ISA molecules formed by physisorption from 1-octanol at a liquid/graphite interface. Image size is 10 × 10 nm^2. The value for ΔL_1 is identical with the one in (a) and corresponds again to interdigitated C_{18}ISA molecules, while the value for ΔL_2 corresponds to the width of the lamella built up by solvent molecules. (d) Molecular model for the two-dimensional packing of C_{18}ISA molecules incorporating 1-octanol molecules and proposed unit cell. The unit cell contains two C_{18}ISA and two 1-octanol molecules. The molecular model represents the area indicated in the STM image.

the molecular model contains two molecules. The unit cell parameters *a*, *b* and α, as indicated in Figure 2, are 0.94 ± 0.05 nm, 3.6 ± 0.3 nm, and 81 ± 2°, respectively. The unit cell data are consistent with the previously reported results for C_{16}ISA.[19] From the data analysis it can be concluded that the molecules are oriented in such a way that hydrogen bond formation between neighboring molecules within the same lamella and between different lamellae is enabled. The alkyl chains of the molecules are interdigitated over the full length of the chains. By the interdigitation of the alkyl chains, a closely packed arrangement of the C_{18}ISA molecules is realized. This closely packed arrangement minimizes the free space per unit area within the monolayer on the graphite surface. This results in a maximum stabilizing van der Waals interaction between the C_{18}ISA molecules on one hand and between the molecules and the graphite surface on the other hand. In this way a stable monolayer with a sufficiently low lateral mobility of the molecules on the surface is assembled. This sufficiently low lateral mobility is a prerequisite in order to perform high-resolution STM imaging.

When, instead of phenyloctane, alcohols with a long alkyl chain such as 1-octanol and 1-undecanol are used as a solvent, solvent molecules are incorporated in the monolayer. An example of this solvent codeposition is presented in Figure 2c where 1-octanol was used. The displayed STM image reveals again the molecular arrangement of the adsorbed molecules with submolecular resolution. Two different lamellar widths can be found in contrast to the case of C_{18}ISA monolayers physisorbed from 1-phenyloctane. The largest lamellar width is identical with the one observed in Figure 2a and is determined by the structure and the packing of the C_{18}ISA molecules. The other lamella consists of only solvent molecules. Its width can be correlated with the length of the alkyl chain of the solvent molecules. The 2D unit cell consists of two C_{18}ISA and two 1-octanol molecules, and the unit cell parameters *a*, *b*, and α are 1.15 ± 0.05 nm, 4.9 ± 0.3 nm, and 81 ± 2°, respectively. An illustrative model is shown in Figure 2d. The C_{18}ISA as well as the 1-octanol molecules are interdigitated. In this case, however, hydrogen bonding between the acid functions of isophthalic acid groups of molecules within a lamella occurs. In addition hydrogen bonding of the other acid function of the isophthalic acid group with the 1-octanol molecules is possible. This results in a monolayer that consists of C_{18}ISA lamellae separated by 1-octanol lamellae.

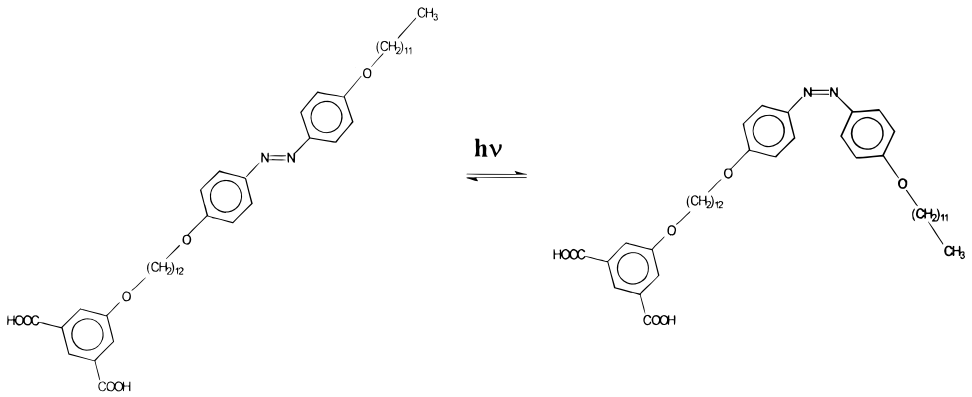

Figure 3. Cis and trans isomers of $C_{12}(AZO)C_{12}ISA$, reagent and product of a reversible photoinduced reaction.

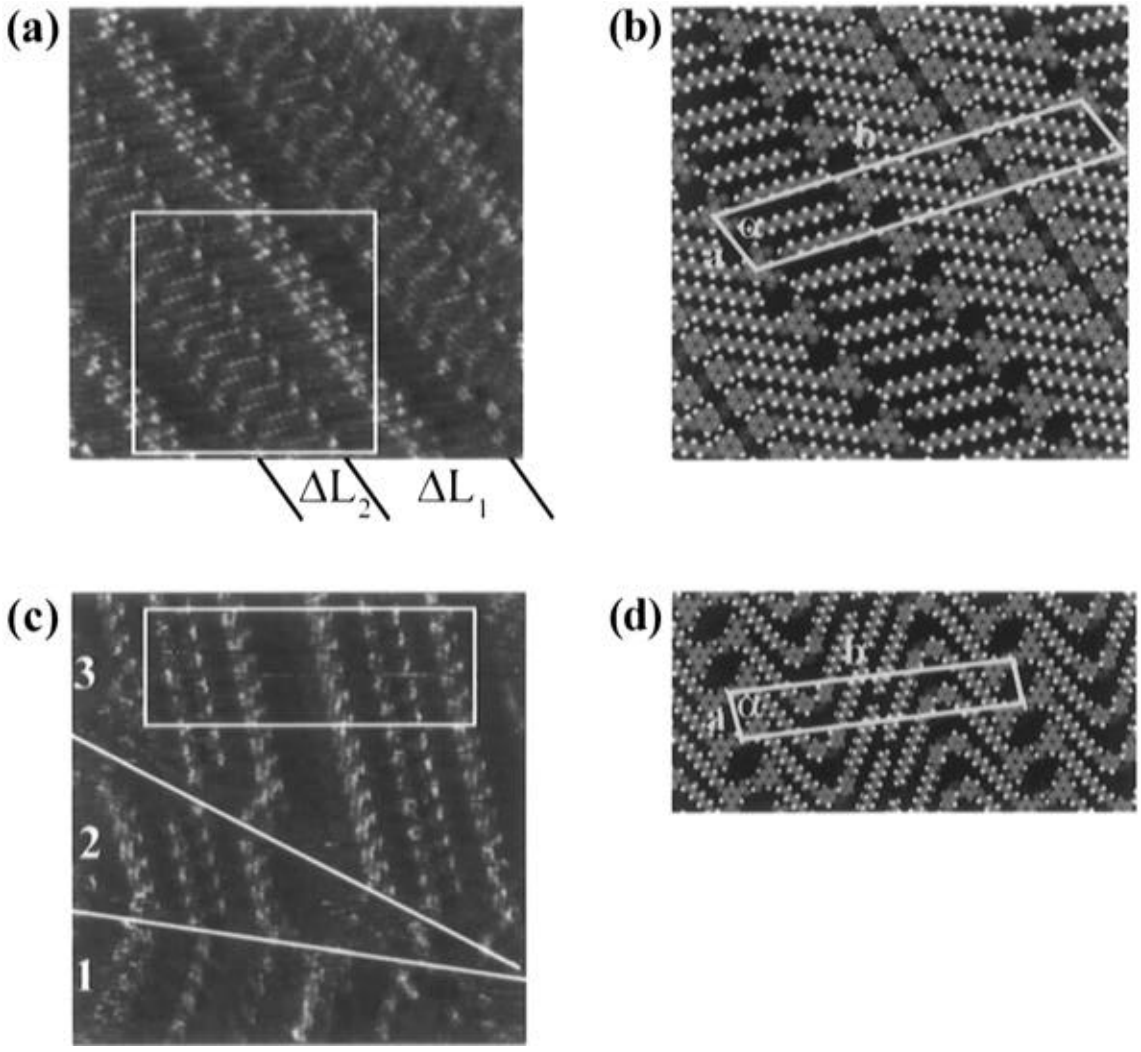

Figure 4. (a) STM image of an ordered monolayer of *trans*-$C_{12}(AZO)C_{12}ISA$ molecules formed by physisorption from 1-undecanol at the liquid/graphite interface. Image size is 13 × 13 nm^2. ΔL_1 is the width of one lamella of interdigitated *trans*-$C_{12}(AZO)C_{12}ISA$ molecules, and ΔL_2 is the width of one lamella of 1-undecanol molecules. (b) Molecular model for the two-dimensional packing of *trans*-$C_{12}(AZO)C_{12}ISA$ molecules incorporating 1-undecanol molecules with proposed unit cell. The unit cell contains two *trans*-$C_{12}(AZO)C_{12}ISA$ molecules and two 1-undecanol molecules. The molecular model represents the area indicated in the STM image. (c) STM image of an ordered monolayer of coexisting *cis*- and *trans*-$C_{12}(AZO)C_{12}ISA$ molecules, which exhibits three domains. The domain boundaries are indicated by white lines. Image size is 13.4 × 13.4 nm^2. The molecular order in domain 1 is identical with the one observed in (a) and corresponds to *trans*-$C_{12}(AZO)C_{12}$-ISA. The molecular order in domains 2 and 3 can be correlated with *cis*-$C_{12}(AZO)C_{12}ISA$. No codeposition with solvent molecules has been observed in the molecular packing of the cis isomers. (d) Molecular model for the two-dimensional packing of *cis*-$C_{12}(AZO)C_{12}ISA$ molecules and proposed unit cell. The unit cell contains two *cis*-$C_{12}(AZO)C_{12}ISA$ molecules. The molecular model represents the area indicated in the STM image.

Preliminary experiments indicate that solvent codeposition might be a rather general phenomenon for these molecules if solvents capable of hydrogen bond formation are used. For example, if a longer chain alcohol such as 1-undecanol is applied as a solvent, a monolayer is assembled that shows a larger separation of the $C_{18}ISA$ lamellae. This indicates that this phenomenon might be used to vary the lamellar structure of a monolayer in a controlled manner. Another important conse-

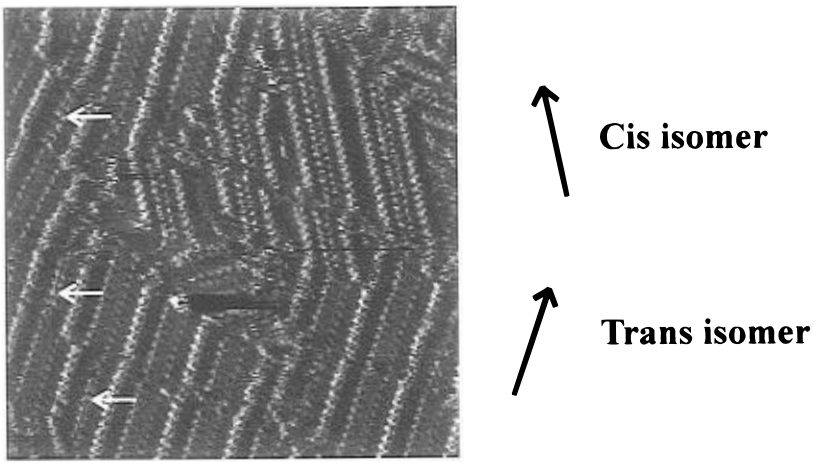

Figure 5. STM image of an ordered monolayer consisting of several domains of $C_{12}(AZO)C_{12}ISA$ molecules. Image size is 40×40 nm^2. Domains consisting of cis and trans isomers can be distinguished by the direction of the lamellae as indicated by the black arrows. The angle between the orientation of the cis and trans lamellae is 30°. Solvent incorporation in the two-dimensional packing of the cis isomer is never observed, in contrast to the monolayers of the trans isomer in which solvent codeposition is mostly found. The white arrows in the STM image indicate the areas within the trans monolayer where no solvent is incorporated.

quence of these results is that the procedure of using small solvent molecules offers an approach for immobilizing these molecules, which cannot be investigated as such at the liquid/graphite interface owing to their high mobility.

Cis−Trans Isomerization. With the aim of imaging the reaction partners of a reversible photoreaction, the cis−trans isomerization of $C_{12}(AZO)C_{12}ISA$ (Figure 3) was investigated.

Upon irradiation with light of an appropriate wavelength, the trans-to-cis isomerization can be induced. To achieve an efficient conversion of the trans to the cis isomer, the irradiation wavelength should match the absorption maximum of the trans isomer. Consequently, the absorption spectrum of a dilute solution of $C_{12}(AZO)C_{12}ISA$ in 1-octanol was recorded. The absorption maximum of the cis and the trans isomers is situated at 317 and 360 nm, respectively. Upon irradiation at 366 nm, a photostationary mixture with a high cis isomer content is reached. The absorbance of this mixture at 360 nm is strongly reduced owing to the increased concentration of the cis isomer. When kept in the dark at room temperature, the cis isomer spontaneously converts to the thermodynamically more stable trans isomer and the absorbance is restored to its original value. Owing to an overlap of the absorption bands, however, it is not possible to prepare solutions containing only cis or trans isomer. In view of its importance for the STM experiments the rate of cis-to-trans isomerization was determined following the increase of absorbance of the trans isomer at 360 nm as a function of time until a photostationary state was reached. The rate constant of cis-to-trans conversion in the absence of light at room temperature amounts to 2.7×10^{-5} s^{-1}.

In Figure 4a a STM image of a monomolecular layer of *trans*-$C_{12}(AZO)C_{12}ISA$ is shown. The layer is prepared by physisorption from a solution of $C_{12}(AZO)C_{12}ISA$ in 1-undecanol that was shielded from light. Hence, the solution should contain merely trans isomers as can be deduced from the absorption spectrum. The closely packed monolayer consists of *trans*-$C_{12}(AZO)C_{12}ISA$ molecules codeposited with 1-undecanol molecules. Distinct bright spots corresponding to the isophthalic acid groups are easily recognized in the image. The somewhat broader bright bands represent the azobenzene moieties. Also, the alkyl chains can be recognized in the image. It was possible to define a unit cell and to create a molecular model shown in Figure 4b. The unit cell parameters *a*, *b*, and α are 0.97 ± 0.10 nm, 6.6 ± 0.4 nm, and 66 ± 4°, respectively. The unit cell contains two $C_{12}(AZO)C_{12}ISA$ and two 1-undecanol molecules. The $C_{12}(AZO)C_{12}ISA$ molecules again interdigitate, and they form lamellae that are separated by lamellae consisting of solvent molecules such as in the case of the $C_{18}ISA$ monolayers.

Figure 4c shows a STM image of a monolayer obtained by physisorption from a photostationary mixture. Three domains can be recognized in this image. The molecular packing in the lower domain is identical with the packing observed in Figure 4a. Consequently, this domain should contain only trans isomer molecules. The patterns observed in the two other domains must originate from a different molecular arrangement. Again, the bright spots correspond to the isophthalic acid groups and the broader bright bands to the azobenzene moieties. The measured lamellar distances and the observed molecular packing correspond to a monolayer of self-assembled cis isomers without solvent codeposition. Figure 4d depicts a 2D unit cell and an illustrative molecular model that can explain the obtained STM data. The unit cell contains two *cis*-$C_{12}(AZO)C_{12}ISA$ molecules, and the parameters *a*, *b*, and α are 1.03 ± 0.10 nm, 6.0 ± 0.4 nm, and 85 ± 4°, respectively. In the molecular model the isophthalic acid groups point toward each other and the alkyl chains are not interdigitated. This results in the specific molecular pattern observed in the two upper domains of Figure 4c. The absence of solvent codeposition is probably due to the spatial orientation of the acid functions in the molecular arrangement of the cis isomer.

Another important aspect of the cis isomer monolayers is the high number of crystallographic defects per unit area found in these layers. Since they are composed of relatively small domains, crystallographic defects in terms of domain boundaries occur relatively often. The small sizes of the domains may result from the fact that owing to the symmetry of the cis isomer and its rather complex arrangement in the monolayers, a defect-free packing is hindered. Interestingly, cis domains were not observed without the presence of trans isomer domains, as shown in Figure 5, and a fixed angle of 30° is always found between the orientation of the cis and trans lamellae. Figure 5 further illustrates that occasionally areas within the *trans*-$C_{12}(AZO)C_{12}ISA$ monolayers can be found where no solvent is incorporated. The coexistence of cis and trans domains correlates not only with the relative amounts of cis and trans isomers in the solution but also with the monolayer stability of the isomers at the liquid/graphite interface.

Similarly, cis−trans isomerization could be induced and their respective domains be imaged by irradiating in situ a droplet of C_{12}(AZO)C_{12}ISA dissolved in 1-undecanol directly on the graphite surface. During imaging, the cis isomer domains disappear with time. Finally, only trans isomer domains could be observed, illustrating the reversibility of the reaction at the liquid/graphite interface.

Conclusion

We have shown that STM can be used to structurally investigate monolayers of C_{18}ISA and C_{12}(AZO)C_{12}ISA with submolecular resolution at a liquid/graphite interface. By employment of solvents capable of hydrogen bond formation, codeposition of solvent molecules is found. The phenomenon of codeposition cannot only be used to stabilize monolayers but it might also be an effective way for immobilizing small solvent molecules that cannot be imaged in monomolecular monolayers owing to their high mobility. By use of codeposition phenomena, it might also be possible to predict the lamellar structure of these monolayers.

We have further demonstrated that both reagent and product of a reversible photoinduced reaction can structurally be identified with submolecular resolution at the liquid/graphite interface. Moreover, images containing both cis and trans monolayers could be obtained.

Acknowledgment. The authors thank FKFO and DWTC for continuing financial support through IUAP-II-16 and IUAP-III-040. S. De Feyter is a predoctoral fellow of the NFWO, and P. Vanoppen thanks the IWT for a predoctoral scholarship.

References and Notes

(1) Rabe, J. P. *Ultramicroscopy* **1992**, *42*−*44*, 41−54.
(2) McGonical, G. C.; Bernhardt, R. H.; Thomson, D. J. *Appl. Phys. Lett.* **1990**, *57*, 28.
(3) Engel, A. *Annu. Rev. Biophys. Chem.* **1991**, *20*, 79.
(4) Frommer, J. *Angew. Chem., Int. Ed. Engl.* **1992**, *31*, 1298−1328.
(5) Rabe, J. P.; Buchholz, S. *Science* **1991**, *253*, 424−427.
(6) Stabel, A.; Heinz, R.; De Schryver, F. C.; Rabe, J. P. *J. Phys. Chem.* **1995**, *99*, 505−507.
(7) Liu, T.-L.; Parakka, J. P.; Cava, M. P.; Kim, Y.-T. *Langmuir* **1995**, *11*, 4205−4208.
(8) Rabe, J. P.; Buchholz, S. *Phys. Rev. Lett.* **1991**, *66*, 2096.
(9) Stevens, F.; Dyer, D. J.; Walba, D. M. *J. Vac. Sci. Technol. B.* **1996**, *14*, 38−41.
(10) Stabel, A.; Heinz, R.; Rabe, J. P.; Wegner, G.; De Schryver, F. C.; Corens, D.; Dehaen, W.; Süling, C. *J. Phys. Chem.* **1995**, *99*, 8690−8697.
(11) Elbel, N.; Roth, W.; Günther, E.; von Seggern, H. *Surf. Sci.* **1994**, *303*, 424−432.
(12) Poulin, J.-C. *Microsc. Microanal. Microstruct.* **1994**, *5*, 351−358.
(13) Heinz, R.; Stabel, A.; Rabe, J. P.; Wegner, G.; De Schryver, F. C.; Corens, D.; Dehaen, W.; Süling, C. *Angew. Chem.* **1994**, *106*, 2154−2157.
(14) Pfaadt, M.; Moessner, G.; Pressner, D.; Valiyaveettil, S.; Boeffel, C.; Müllen, K.; Spiess, H. W. *J. Mater. Chem.* **1995**, *5*, 2265−2274.
(15) van Genderen, M. H. P.; Pfaadt, M.; Möller, C.; Valiyaveettil, S.; Spiess, H. W. *J. Am. Chem. Soc.* **1996**, *118*, 3661−3665.
(16) Valiyaveettil, S.; Enkelmann, V.; Müllen, K. *J. Chem. Soc., Chem. Commun.* **1994**, 2097−2098.
(17) Enkelmann, V.; Valiyaveettil, S.; Moessner, G.; Müllen, K. *Supramol. Sci.* **1995**, *2*, 3.
(18) Valiyaveettil, S.; Enkelmann, V.; Moessner, G.; Müllen, K. *Makromol. Chem., Macromol. Symp.* **1996**, *102*, 165.
(19) Eichhorst-Gerner, K.; Stabel, A.; Declercq, D.; Rabe, J. P.; Moessner, G.; Valiyaveettil, S.; Enkelmann, V.; Müllen, K. *Angew. Chem., Int. Ed. Engl.* **1996**, *35*, 1492−1495.
(20) Valiyaveettil, S.; Gans, C.; Klapper, M.; Gereke, R.; Müllen, K. *Polym. Bull.* **1994**, *34*, 13.
(21) Lazzaroni, R.; Calderone, A.; Lambin, G.; Rabe, J. P.; Brédas, J. *Synth. Met.* **1991**, *41*−*43*, 525.

JP962737+